Bio-Design and Manufacturing (2023) 6:451–463
https://doi.org/10.1007/s42242-023-00242-6

RESEARCH ARTICLE

3D printing of personalized polylactic acid scaffold laden with GelMA/autologous auricle cartilage to promote ear reconstruction

Xingyu Gui[1,4] · Zhiyu Peng[2] · Ping Song[1,4] · Li Chen[3] · Xiujuan Xu[1,4] · Hairui Li[5] · Pei Tang[5] · Yixi Wang[5] · Zixuan Su[1,4] · Qingquan Kong[6] · Zhenyu Zhang[5] · Zhengyong Li[5] · Ying Cen[5] · Changchun Zhou[1,4] · Yujiang Fan[1,4] · Xingdong Zhang[1,4]

Received: 21 November 2022 / Accepted: 7 March 2023 / Published online: 27 April 2023

Abstract

At present, the clinical reconstruction of the auricle usually adopts the strategy of taking autologous costal cartilage. This method has great trauma to patients, poor plasticity and inaccurate shaping. Three-dimensional (3D) printing technology has made a great breakthrough in the clinical application of orthopedic implants. This study explored the combination of 3D printing and tissue engineering to precisely reconstruct the auricle. First, a polylactic acid (PLA) polymer scaffold with a precisely customized patient appearance was fabricated, and then auricle cartilage fragments were loaded into the 3D-printed porous PLA scaffold to promote auricle reconstruction. In vitro, gelatin methacrylamide (GelMA) hydrogels loaded with different sizes of rabbit ear cartilage fragments were studied to assess the regenerative activity of various autologous cartilage fragments. In vivo, rat ear cartilage fragments were placed in an accurately designed porous PLA polymer ear scaffold to promote auricle reconstruction. The results indicated that the chondrocytes in the cartilage fragments could maintain the morphological phenotype in vitro. After three months of implantation observation, it was conducive to promoting the subsequent regeneration of cartilage in vivo. The autologous cartilage fragments combined with 3D printing technology show promising potential in auricle reconstruction.

Xingyu Gui and Zhiyu Peng have contributed equally to this work.

✉ Changchun Zhou
changchunzhou@scu.edu.cn

✉ Yujiang Fan
yujiang.fan@163.com

1 National Engineering Research Center for Biomaterials, Sichuan University, Chengdu 610064, China

2 Department of Thoracic Surgery, West China Hospital, Sichuan University, Chengdu 610041, China

3 Analytical and Testing Center, Sichuan University, Chengdu 610064, China

4 College of Biomedical Engineering, Sichuan University, Chengdu 610064, China

5 Department of Burn and Plastic Surgery, West China Hospital, Sichuan University, Chengdu 610041, China

6 Department of Orthopedics, West China Hospital, Sichuan University, Chengdu 610041, China

Graphic abstract

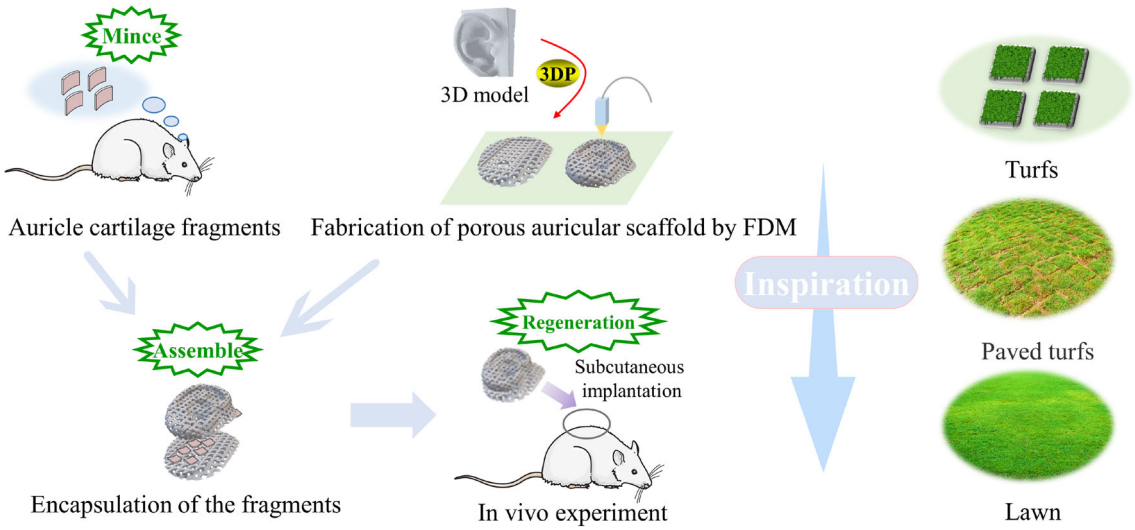

Keywords Microtia · 3D printing · Polylactic acid (PLA) polymer scaffolds · Gelatin methacrylamide · Cartilage reconstruction

Introduction

Auricle defect caused by congenital disease and accidental trauma is a challenging clinical problem due to the complex anatomical shape of the auricle [1, 2]. An abnormality of the auricle, also known as microtia, can cause emotional disorders in patients, especially in children, and can affect hearing in the presence of the auditory canal [3, 4]. At present, the main therapeutic methods for auricle defects include ear reconstruction with autologous costal cartilage and ear reconstruction with artificial materials [5, 6]. The former, however, causes damage to the donor site and requires excellent surgical skills to achieve good esthetic outcomes [7]. In addition, artificial auricle materials such as Medpor are substitutes for autologous materials in cartilage transplantation, which carry a high risk of infection [8]. In other words, although the treatment of auricle defects has been successful in some aspects, these methods have limitations.

Tissue engineering of auricular cartilage has great potential, providing an effective alternative strategy for auricle reconstruction surgery [9–11]. This method can inoculate cells into biocompatible or biodegradable scaffolds to repair tissue defects [12, 13]. However, scaffold-delivered cell therapy has some limitations in clinical transformation, such as limited sources, difficulty in predicting long-term efficacy, and high cost [14]. In addition, the phenotype of the chondrocytes obtained after isolation and monolayer expansion of the chondrocytes is severely affected, which should not be ignored compared to newly isolated chondrocytes [15]. Studies have shown that repairing cartilage defects by autologous cartilage fragments is another method [16, 17]. Cartilage fragments are flexible in application and are also used in ear reconstruction, nose surgery and chest wall defect filling [18, 19]. However, microtia or partial ear defects do not have sufficient cartilage available in situ to produce an ear anatomical structure to satisfy esthetic requirements. In fact, a well-designed tissue-engineered scaffold may do a better job of keeping the auricle in shape than a dimensional ear scaffold with autogenous costal cartilage meticulously sculpted and assembled by a skilled physician [20].

Relating to the field of tissue engineering, three-dimensional (3D) printing is widely used in the fabrication of tissue-engineered scaffolds due to its flexible preparation of complex structures [21–24]. 3D printing can quickly reconstruct a personalized 3D model of a patient's ear to directly improve patient outcomes. More importantly, it can create porous structures that are difficult to fabricate with traditional techniques. In addition, while designing and fabricating auricle prostheses using 3D printing technology, sufficient hardness and strength should be considered to support the shape [1, 25]. Synthetic polymers such as polylactic acid (PLA), polycaprolactone and polyethylene have been widely used in cartilage repair due to their superiority in mechanical properties, biocompatibility and biodegradability [25–27]. However, these artificial polymers lack sufficient active groups and cannot carry cells or bioactive

molecules for tissue regeneration [28]. Hydrogels have excellent biodegradability and biocompatibility as well as good similarity to the tissue environment and are thus considered to be biomaterials with great potential in use as tissue engineering scaffold materials [29]. Among these hydrogel materials, photo-crosslinked gelatin methacrylamide (GelMA) hydrogels have basic properties similar to those of the natural extracellular matrix and show potential value for tissue engineering cartilage constructs [30–32].

In this work, 3D-printed PLA polymer scaffolds laden with GelMA hydrogel/autologous ear cartilage fragments with accurate appearance were used to promote auricle reconstruction. Different sizes of rabbit cartilage fragments were encapsulated in GelMA hydrogel, and the effect of size on cartilage fragmentation was evaluated in vitro. Then, in vivo experiments were carried out to study the reconstruction ability of these scaffolds. After three months of implantation, it was observed that chondrocytes in the cartilage fragments could maintain the morphological phenotype, which was conducive to promoting the subsequent regeneration of auricle cartilage. This novel combined treatment shows promising potential in auricle reconstruction.

Materials and experiments

Preparation of gelatin methacrylamide (GelMA)

As shown in Fig. 1, an approach to fabricate autologous ear cartilage graft debris combined with a 3D-printed PLA scaffold to repair auricle defects was proposed. Type A pork skin gelatin (VWR, USA) was dissolved in pH 9 sodium carbonate-bicarbonate (CB) buffer. Methacrylic anhydride (MA) was added to the gelatin solution at an MA/gelatin feed ratio of 0.075/1 and stirred at 50 °C for 1 h. The solution was then dialyzed with ultrapure water for three days using a dialysis tube. Finally, the resulting solution was frozen at −20 °C for 24 h and freeze-dried for 48 h. The lyophilized GelMA was stored at −20 °C for further use.

Characterization of GelMA

To calculate the degree of methacrylation (DM), 10 mg GelMA and 10 mg gelatin were dissolved in 0.5 mL D_2O and analyzed using a 400-Hz nuclear magnetic resonance (Bruker AVANCE AV II-400 MHz, Switzerland). The obtained GelMA and gelatin ^{1}H-nuclear magnetic resonance (^{1}H-NMR) data were subjected to baseline correction, and the lysine methylene proton peak at 2.8–2.95 ppm (1 ppm=1×10^{-6}) was normalized with reference to the peak at 7.1–7.4 ppm. The DM of GelMA was calculated by the following formula:

$$\mathrm{DM} = \left[\int \mathrm{Gelatin}(2.8\ \mathrm{ppm} - 2.95\ \mathrm{ppm}) - \int \mathrm{GelMA}(2.8\ \mathrm{ppm} - 2.95\ \mathrm{ppm})\right] \cdot \left[\int \mathrm{Gelatin}(2.8\ \mathrm{ppm} - 2.95\ \mathrm{ppm})\right]^{-1} \times 100\%. \quad (1)$$

GelMA was dissolved in ultrapure water at 15% (0.15 g/mL) with 0.25% (0.0025 g/mL) of the photoinitiator lithium phenyl (2,4,6-trimethylbenzoyl) phosphinate (LAP) and then cured by ultraviolet light at 10 mW/cm^2. The freeze-dried GelMA hydrogel was sprayed with gold, and the microstructure was characterized by a Phenom table-top scanning electron microscopy (SEM, ProX-SE, Phenom, Netherlands). The rheological properties of GelMA were tested by a rheometer (MCR302, Anton Paar, Austria). The viscosity of the 5% (0.05 g/mL) GelMA solution was measured by cooling from 40 to 10 °C at a constant shear rate of 50 s^{-1} with a rate of 4 °C /min. The shear rate-viscosity test was carried out at 25 °C, and the shear rate increased from 1 s^{-1} to 50 s^{-1}. A dynamic mechanical analyzer (DMA, TA Instruments, Q-800, USA) was used to test the storage modulus (G') and loss modulus (G'') of the GelMA hydrogel in the multi-frequency mode with a fixed frequency band of 1–10 Hz.

Fabrication and characterization of porous PLA scaffold

PLA (Jinan Daigang Biomaterial Co., Ltd., Jinan, China, M_v=200,000) was used to fabricate porous PLA scaffolds by a fused deposition modeling 3D printer. After spraying gold on the surface of the samples, the morphology of the porous PLA scaffold was observed by scanning electron microscopy (SEM, JSM-5900LV, JEOL, Japan). An accelerated degradation experiment was performed in vitro to evaluate the degradation properties of PLA. The polylactic acid was placed into a 50 mL centrifuge tube, submerged in phosphate buffered saline (PBS) medium, and then incubated in an incubator at 70 °C. At various time points (0, 1, 3, 7, 12, and 17 days), samples were removed and sucked dry. The molecular weight of the sample was measured by gel permeation chromatography (GPC, Waters Breeze2, USA), and PLA was dissolved by high performance liquid chromatography (HPLC) chloroform. The injection volume of each sample was 100 μL with a 30 min operation. Subsequently, the samples degraded for 17 days were characterized by SEM. The mechanical properties of porous PLA scaffolds were tested by an electronic universal machine (INSTRON, USA). The standard cylinder (Φ7.5 mm×15 mm) scaffolds were stressed at a crosshead speed of 1 mm/min.

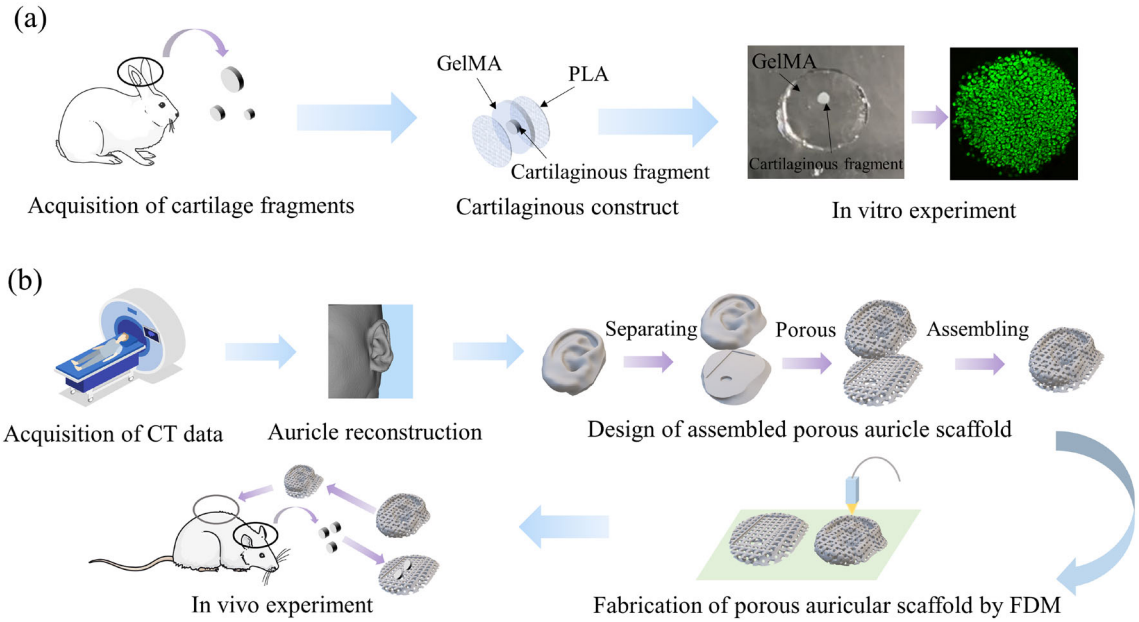

Fig. 1 Experimental overview of ear cartilage fragments combined with a 3D-printed porous auricle scaffold in vivo and in vitro. **a** Activity evaluation of rabbit ear cartilage fragments in vitro. **b** In vivo cartilage fragments combined with a 3D-printed PLA scaffold to reconstruct the auricle. GelMA: gelatin methacrylamide; PLA: polylactic acid; CT: computed tomography; FDM: fused deposition modeling

Extraction of cartilage fragments and in vitro experiments

Cartilage grafts were taken from ears of New Zealand white rabbits. First, wipe the auricle with iodophor and peel off the skin and fibrous tissue, and then wash and soak in PBS containing 10% penicillin–streptomycin. The auricle was used to extract the cartilage fragments with circular hole cutters with diameters of 1, 2, and 3 mm. Then, the cartilage fragments, PLA porous slices and 5% (0.05 g/mL) GelMA solution were cured together in a 2 mm×8 mm silicone mold. Finally, the cartilage fragment/GelMA mixtures were cultured in Minimum Essential Medium (MEM) Alpha modification medium with 10% serum, 1% penicillin–streptomycin and 0.009% vitamin C. Live cells and dead cells were stained with fluorescein diacetate/propyl iodide (FDA/PI) (Sigma, USA), and cell proliferation was detected by cell counting kit-8 (CCK-8) (Beyotime, Shanghai, China). Then, the cells were fixed and stained with 4',6-diamidino-2-phenylindole (DAPI)/Palloidin (Sigma, USA) and finally observed by a laser confocal microscope (Zeiss, SM 800, Germany).

In vivo experiments

Three-month-old female Sprague–Dawley (SD) rats were purchased from the Experimental Animal Center of Sichuan University. All experiments were approved by the Animal Care and Use Committee of Sichuan University. Before the experiment, rats were anesthetized by intraperitoneal injection of 1% sodium pentobarbital at a dose of 0.4 mL/100 g. The ears of the rats were wiped with iodophor, and the auricles were removed with surgical scissors. Then, the skin and fibrous tissue were peeled off on an ultraclean table, and cartilage fragments were extracted with surgical scissors. The 3D-printed PLA assembled scaffold was sterilized and used to load cartilage fragments, and the GelMA solution was poured into the scaffold to encapsulate the cartilage fragments. Subsequently, the 3D-printed PLA scaffold was fixed by sutures. Through optimized screening of the cartilage fragments in vitro, we only chose 1 mm cartilage fragments as experimental specimens to study the long-term maintenance of chondrocyte activity and auricle shape. These scaffolds were implanted subcutaneously in anesthetized rats and carried in their bodies for 1 month, 2 months, and 3 months. The rats were sacrificed by cervical dislocation at the experimental times, and the scaffolds were removed and fixed with 4% paraformaldehyde for histological analysis.

Histological staining

The scaffold grafts were embedded in paraffin, and the embedded scaffolds were cut into 5 μm sections using a Leica polycut (Leica, SM 2500e, Germany). The sections were stained with hematoxylin and eosin (H&E) and toluidine blue for histological analysis.

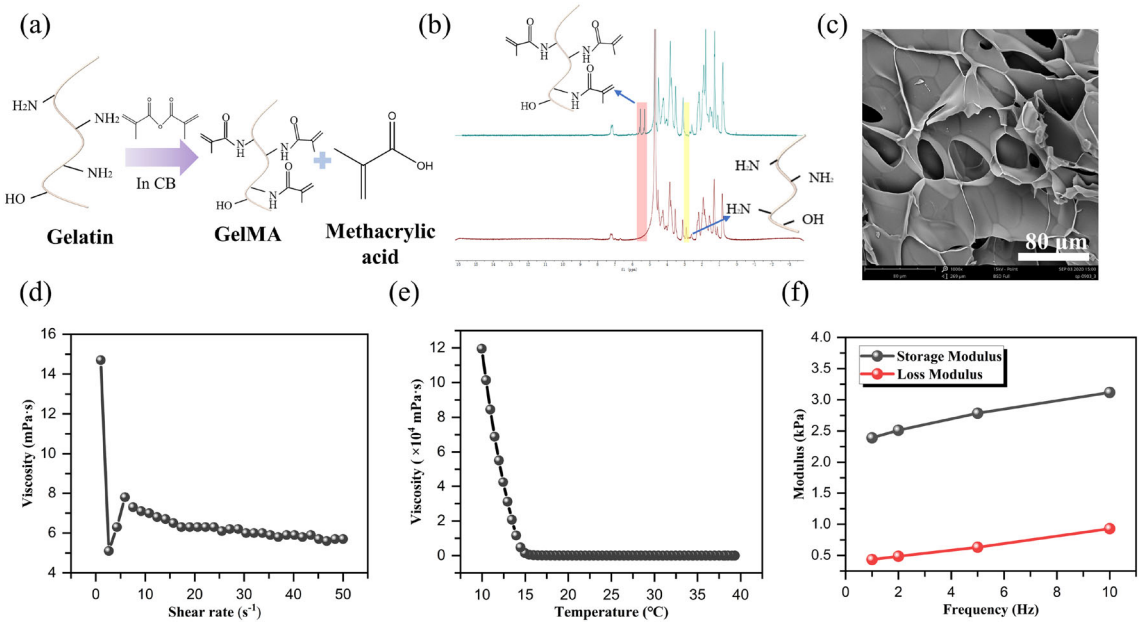

Fig. 2 Fabrication of GelMA and characterization of GelMA hydrogel. **a** Schematic diagram of GelMA synthesis. **b** Comparison of gelatin and GelMA ^{1}H-NMR spectra. **c** SEM images obtained from lyophilized GelMA. **d** Shear thinning properties of 5% (0.05 g/mL) GelMA solution. **e** Temperature response of the viscosity of GelMA solution. **f** DMA analysis for GelMA hydrogel with frequency dependency. GelMA: gelatin methacrylamide; ^{1}H-NMR: ^{1}H-nuclear magnetic resonance; SEM: scanning electron microscopy; DMA: dynamic mechanical analyzer

Statistical analysis

At least three samples were tested in each experiment. The data are expressed as the mean±standard deviation (SD). The statistically significant difference level was set as $*p<0.05$, $**p<0.01$, $***p<0.001$, and $****p<0.0001$.

Results and discussion

GelMA characterization

GelMA was synthesized by methacrylic anhydride substitution of the lysine amino of gelatin (Fig. 2a). The resulting methacrylic acid results in protonation of the free amino group and inhibits further reaction with methacrylic anhydride. As shown in Fig. 2b, the appearance of the acrylic proton peak of the methacrylamide graft and the weakening of the characteristic peak of the lysine methylene proton indicate the successful synthesis of GelMA. According to Eq. (1), the degree of methacrylation of GelMA reached 82.74% under low amounts of methacrylate anhydride. Figure 2c shows the microstructure of the GelMA hydrogel observed by SEM. SEM images reveal that the hydrogel has a homogeneous and interconnected porous structure, which is conducive to the transport of nutrients and the maintenance of biomimetic extracellular matrix (ECM). This may be critical for the life support of chondrocytes in cartilage fragments. As is shown in Fig. 2d, as the shear rate gradually increased to 50 s^{-1}, the GelMA solution exhibited shear thinning, a property that makes it easy to push out of the syringe and inject into the porous scaffold for encapsulation of cartilage fragments. In addition, as shown in Fig. 2e, after the GelMA solution was cooled from 40 to 10 °C, the viscosity of the solution increased rapidly at approximately 15 °C, indicating the physical crosslinking of gelatin. It is expected that this GelMA solution, which maintains a low viscosity at room temperature, can quickly fill the pores of the scaffold. From the DMA analysis of the GelMA hydrogel in Fig. 2f, the storage modulus is as high as 3.118 kPa. Although chondrocytes were not isolated from the fragments in further studies, the lower modulus of hydrogels may maintain the chondrocyte phenotype. In vitro studies have shown that there are complex interactions between cells and materials in a 3D culture environment, in which a soft matrix can promote cell aggregation as well as spherical and cartilage formation [33, 34]. Thus, this low-stiffness hydrogel has the potential to promote chondrogenesis and the cartilage phenotype.

Characterization of porous PLA scaffolds and degradation of PLA

Tissue engineering techniques provide a promising method for auricle reconstruction of microtia. Although tissue-engineered scaffolds include scaffolds, cells and growth

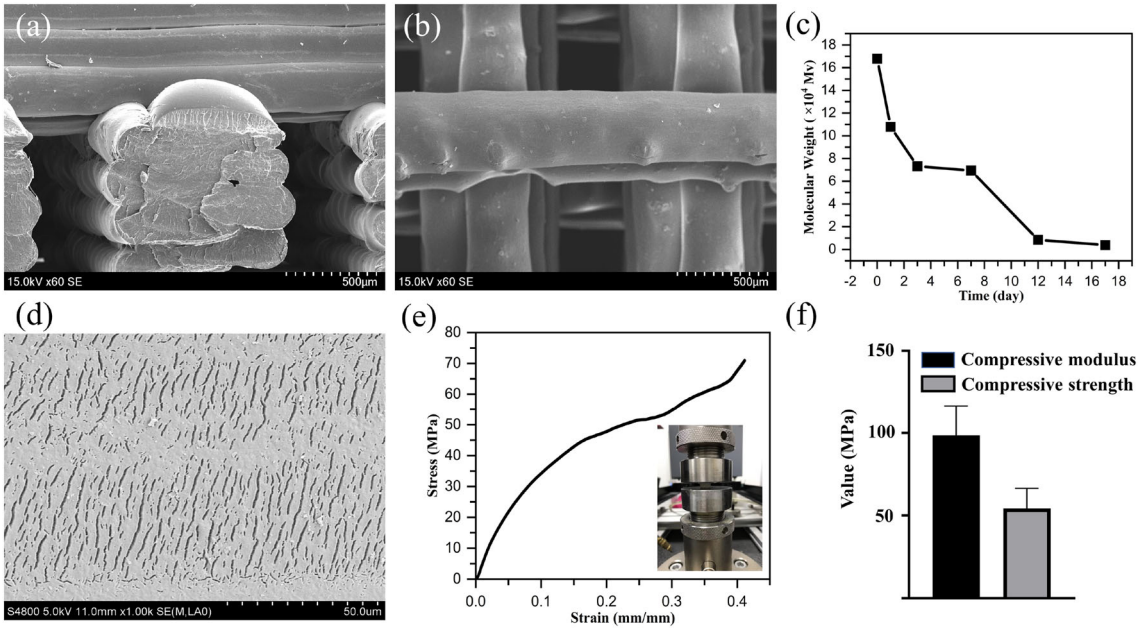

Fig. 3 Micromorphology of the porous PLA scaffold and evaluation of the PLA degradation. **a, b** SEM images of the porous PLA scaffold. **c** The degradation curve of the PLA. **d** The micromorphology of the PLA after 17 days of degradation. **e** The stress–strain curve of the porous PLA scaffold. **f** The compressive modulus and compressive strength of the porous PLA scaffold. PLA: polylactic acid; SEM: scanning electron microscopy

factors, the clinical transformation of cells and growth factors remains to be solved. Therefore, the material properties and forming methods of scaffolds are of great significance for tissue repair. According to the three-dimensional model of the healthy auricle obtained from the patient's computed tomography (CT) data, PLA can be used as the material for 3D printing to fabricate the auricle scaffold. Figures 3a and 3b show the microstructures of porous PLA scaffolds prepared by fused deposition modeling (FDM) technology. Although PLA is a polymer with poor hydrophobicity and tissue integration, the pore structure of the scaffold allows the growth of cells and tissues to form mechanical tissue integration [12].

Whether in vivo degradation of polylactic acid scaffolds can maintain the mechanical strength and shape of the reconstructed auricle is a clinical concern. The correlation between molecular weight and degradation time is shown in Fig. 3c. At the initial stage of degradation, the molecular weight of PLA decreased rapidly and then slowed down. After 17 days of accelerated degradation in vitro, a large number of cracks appeared on the surface of the PLA (Fig. 3d). The experimental evaluation of accelerated degradation in vitro showed that polylactic acid degraded slowly in vivo. PLA porous scaffolds provide mechanical support for cartilage regeneration to maintain esthetic appearance. Moreover, the slow hydrolysis of PLA can provide sufficient regeneration time for auricle reconstruction and gradual space replacement for scaffold degradation. Previous studies have shown that the degradation of PLA may result in inflammation [35]. However, PLA and its derivative hydrogels promoted the production of cartilage-specific extracellular matrix through ester hydrolysis [36, 37]. Furthermore, studies have shown that polylactic acid has a lower degradation rate and milder inflammatory response in vivo than polymers such as polyglycolic acid (PGA) and poly(lactic-co-glycolic acid) (PLGA) [10, 32]. Subsequently, the mechanical properties of the porous PLA scaffold were evaluated. As shown in Fig. 3e, the stress–strain curve of the porous PLA scaffold showed an initial rigid response. With increasing strain, the porous structure collapsed and was compacted, and the compressive strength increased continuously. According to the linear yield response, the compressive modulus and compressive strength of the porous scaffold were (98.73±17.86) MPa and (54.26±12.25) MPa, respectively (Fig. 3f). Therefore, the porous scaffold has sufficient mechanical properties to maintain the shape of the auricle and provide mechanical support for cartilage regeneration.

Extraction of cartilage fragments and in vitro experiments

There are many challenges with cells in tissue-engineered scaffolds, such as source restriction, dedifferentiation and disease infection. Autologous cartilage fragments have strong biological potential and clinical application value

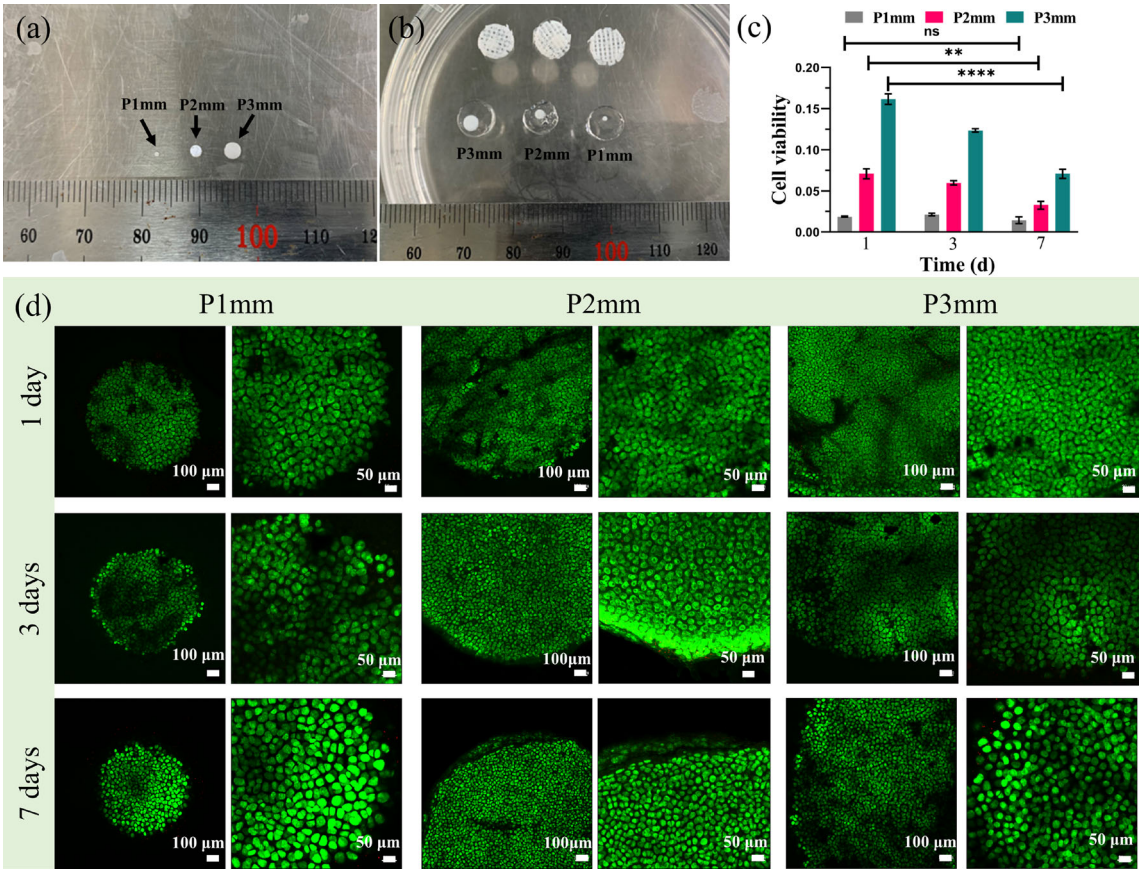

Fig. 4 Extraction of cartilage fragments and evaluation of cartilage graft activity in vitro. **a** Cartilage fragments with dimensions of 1, 2 and 3 mm, which were named P1mm, P2mm and P3mm, respectively. **b** Encapsulation of cartilage fragments and PLA porous slices using GelMA hydrogel. **c** Quantification of cartilage fragment viability by CCK-8. **d** Laser-scanning confocal images of live (green) and dead (red) stains. PLA: polylactic acid; GelMA: gelatin methacrylamide; CCK-8: cell counting kit-8

because they have autologous and non-dedifferentiated chondrocytes and are available from residual ear cartilage of patients with microtia [38]. As shown in Fig. 4a, ear cartilage fragments with different sizes were extracted from rabbit auricles with circular hole cutters. Subsequently, in Fig. 4b, cartilage fragments of different sizes and porous PLA sheet scaffolds were encapsulated into GelMA hydrogels to form sandwich complexes to evaluate their biological properties in vitro. Figure 4c presents the viability of the cartilage fragments of different sizes quantitatively measured by CCK-8. Since larger cartilage fragments have more active chondrocytes, the cell viability value of 3 mm cartilage fragments on the first day is much greater than that of 1 mm and 2 mm cartilage fragments. Similarly, the sequencing of cell viability values in cartilage fragments at day 3 and day 7 was related to fragment size. However, it is worth noting that compared with 1 mm cartilage fragments, the viability of 2 mm and 3 mm cartilage fragments decreased significantly with increasing culture time. Although the thickness of the cartilage fragments was slightly different, it still indicates that smaller cartilage fragments can maintain higher cell viability in vitro. The ECM of cartilage consists of 70%–80% of water, and nutrients are delivered to deep chondrocytes through infiltration [39]. It can be speculated that the chondrocytes in smaller cartilage fragments may have easier access to the required substances. Furthermore, after 1, 3 and 7 days in vitro, laser confocal live and dead images of cartilage fragments were obtained (Fig. 4d). After 7 days of culture, there was almost no large-area death of chondrocytes. Almost every chondrocyte showed a rounded morphology predicting a good phenotype. However, in contrast to the CCK-8 results, chondrocyte activity or obvious proliferation in cartilage fragments of different sizes could not be observed in the image. This may be explained by the fact that cartilage fragments of different sizes may induce different degrees of chondrocyte activity. In addition, in contrast to other cells, some cells in the cartilage exhibit low metabolic activity [40].

Figure 5 shows the chondrocyte morphology images of cartilage fragments obtained from laser confocal microscopy. Some chondrocytes may not be well stained or blocked from

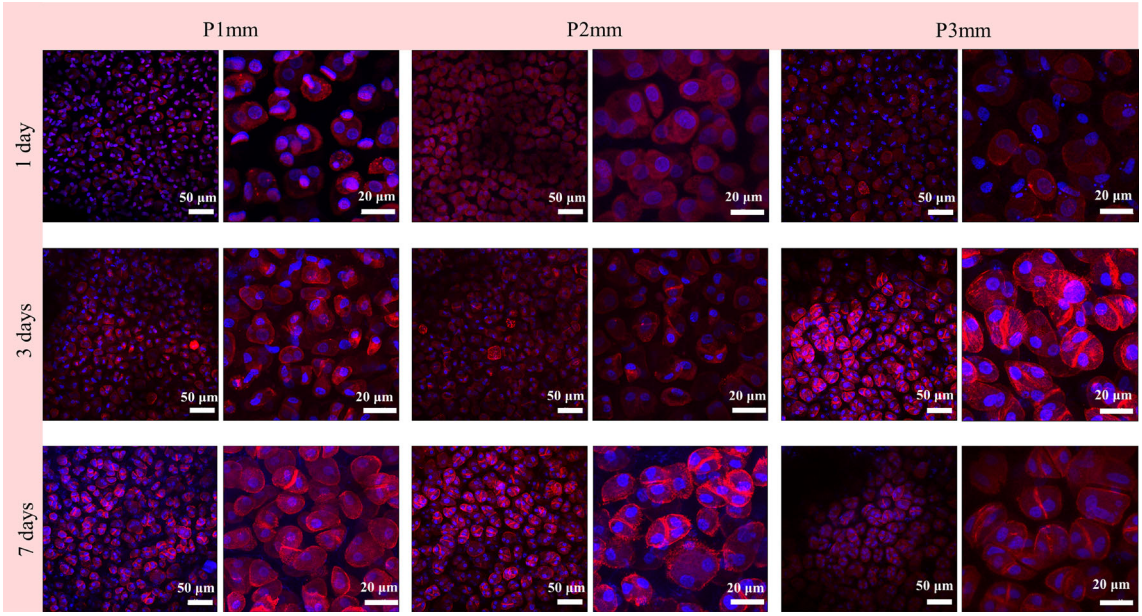

Fig. 5 Laser-scanning confocal images of cartilage fragments with different sizes stained by rhodamine-phalloidin/DAPI. DAPI: 4',6-diamidino-2-phenylindole

lasers due to the interference of the cartilage matrix and partially unstripped fibrous tissue, resulting in blurred and distorted images. The cartilage cytoskeleton in the cartilage fragments was clear, with actin in red and nuclei in blue. Chondrocytes take on a rounded morphology, which is a characteristic of the chondrogenic phenotype. Although there was no significant difference in morphology between cartilage fragments with different sizes, cartilage fragments with larger sizes had more isogenous groups, and the chondrocytes in the isogenous groups were more mature and metabolized slowly. Therefore, in view of the better activity of smaller cartilage fragments in the in vitro evaluation, 1 mm cartilage fragments were selected for further study.

In vivo experiment of 3D-printed scaffolds encapsulating autogenous ear cartilage fragments

Rat ear cartilage was extracted and prepared into smaller cartilage fragments and combined with a 3D-printed auricle scaffold. The environment under which the subcutaneous transplantation of the scaffold was performed can truly simulate the environment of clinical auricle reconstruction. As shown in Fig. 6a, cartilage fragments were wrapped by GelMA hydrogels and solidified in the grooves of the scaffold. The scaffold was assembled and fixed with sutures and then implanted subcutaneously (Figs. 6b and 6c). Three months after implantation, there were no damage to the skin surface and no obvious inflammatory infection (Fig. 6d). The scaffolds were covered with blood vessels and tissues without obvious tissue lesions, and the structure of the auricle scaffolds remained intact without obvious degradation (Figs. 6e and 6f). The vascularization of tissue-engineered ear scaffolds is of great significance and provides nutrients, growth factors and metabolic channels for cartilage tissues [39]. However, studies have shown that cartilage is a kind of nonvascular tissue. The lipid and oxygen brought by blood vessels penetrating into the cartilage may lead to a poor cartilage phenotype and even hypertrophy to form calcified cartilage [15, 41]. This biodegradable GelMA hydrogel temporarily may prevent vascular invasion, and blood vessels provide materials for cartilage tissues through osmosis, which is also a normal form of cartilage metabolism.

The biological rationale behind loading cartilage fragments intended for auricle reconstruction is that sufficient amounts of activated autologous cartilage are available for in situ repair [38]. Figure 7a illustrates the cutting method of the auricle scaffold and shows the grooves loaded with cartilage fragments. Figure 7b shows the in vivo results at each time point of 1, 2, and 3 months to evaluate cartilage tissue formation in the auricle scaffold. The chondrocytes in the cartilage fragments were round and embedded in the eosinophilic extracellular matrix. Some studies have shown that breaking the cartilage into small pieces may increase the production of extracellular matrix [42]. In addition, studies have reported that chondrocytes grow into scaffolds and found that there is an inverse relationship between the size of cartilage fragments and growth efficiency [43]. There was no obvious expansion of chondrocytes in cartilage fragments three months after implantation. It seems that chondrocytes

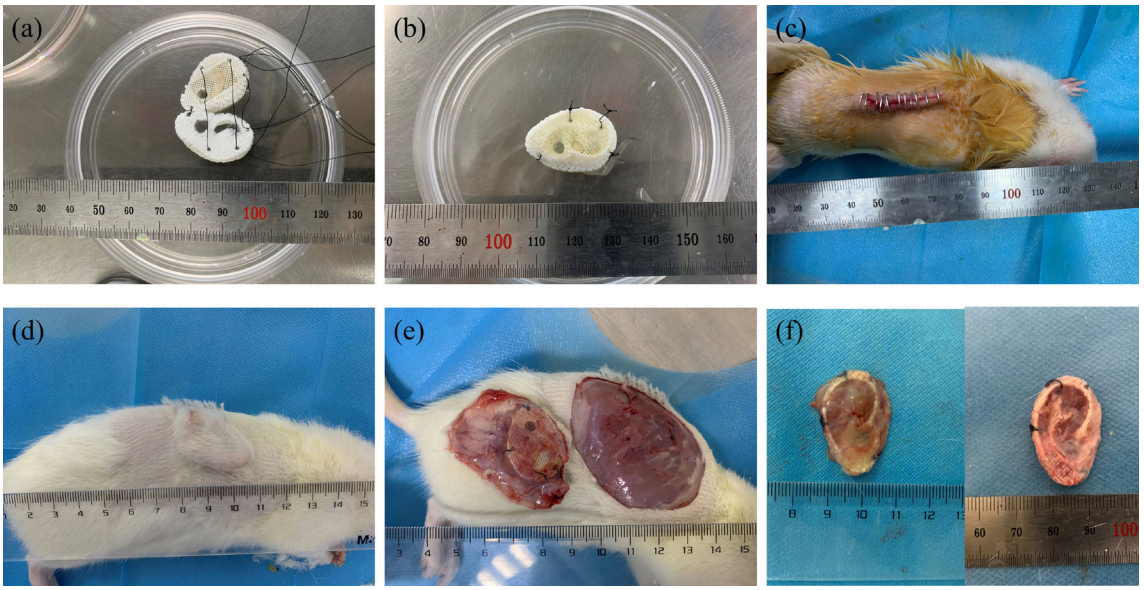

Fig. 6 Autologous ear cartilage fragments in vivo. **a** Encapsulation of cartilage fragments. **b** Assembling and positioning of the 3D-printed porous PLA auricle scaffold. **c** Appearance when the auricle scaffold was just subcutaneously implanted in a rat. **d** Appearance three months after the auricle scaffold implantation. **e** Photographs of the auricle scaffold subcutaneously implanted in a rat after three months. **f** Scaffold complexes loaded with cartilage fragments after three months. PLA: polylactic acid

only divide and proliferate in the width direction. Although it is possible to effectively induce the migration and proliferation of chondrocytes in cartilage fragments through tissue fragmentation, whether this migration and proliferation are limited by the perichondrium remains to be studied.

As shown in Fig. 8, similarly, chondrocytes in toluidine blue-stained sections showed a round shape, indicating a good phenotype. The cartilage matrix was stained purple blue in toluidine blue. Although the direct implantation of cartilage fragments avoids the in vitro monolayer expansion procedure that may lead to dedifferentiation, it is still possible that the chondrocytes deviate from their original characteristics due to the increase in cell division times.

Minced cartilage implantation is a very attractive method in the treatment of articular cartilage because of its simple operation, low cost and good therapeutic effect [44]. The autologous cartilage tissue used in this method expresses strong biological potential and is rich in non-dedifferentiated chondrocytes without immunogenicity. In addition, residual auricle tissues that can be used to prepare cartilage fragments are available from patients with microtia. 3D printing has attracted extensive attention because of its ability to produce personalized tissue-engineered scaffolds, which is also of great value in auricle reconstruction. It can be predicted that autologous ear cartilage fragments combined with 3D-printed tissue-engineered scaffolds seem to have a great potential for application in auricle reconstruction. Figure 9 shows the inspiration from lawn planting to encapsulate ear cartilage fragments with 3D printing to reconstruct the auricle. A turf block consists of short grass and soil connected by its roots to form a modular lawn of a certain area and eventually a whole lawn. Based on this process, we propose to cut the residual auricle tissue of patients with microtia into small fragments similar to turfs. The cartilage fragments are then encapsulated in a 3D-printed auricle scaffold using GelMA hydrogels. It was reported that the process of chondrocyte growth from debris to plastic can be observed when articular cartilage fragments are cultured in cartilage formation medium [45]. In addition, compared with isolated chondrocytes, shredded cartilage showed better cell migration and proliferation and higher glycosaminoglycan content, which showed that shredded cartilage had good cell proliferation and matrix regeneration ability [46]. Cartilage fragments have the potential to regenerate cartilage tissues through cell migration, proliferation and matrix production, which is similar to how turf can fuse and grow into lawns after a period of time. However, it needs to be clarified that according to the in vivo experimental results, there seems to be no obvious migration of chondrocytes from the fragments. To speak more strictly, there is no expected large-scale migration and proliferation of chondrocytes, even in sections with suspected cartilage migration and proliferation. It is possibly because the membranes or hydrogels are not removed that the migration and proliferation of the cells are blocked. Despite that, however, according to the experimental results, the cells in the cartilage fragments still have a good phenotype and cartilage matrix maintenance. Finally, the implantation of autologous cartilage fragments combined

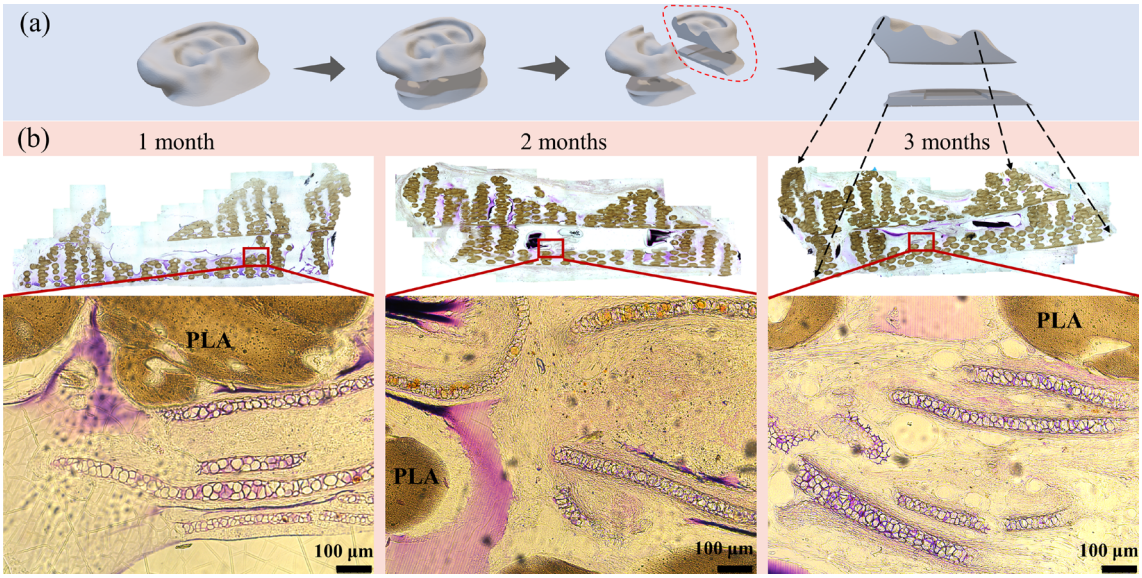

Fig. 7 Histological analysis of the autologous ear cartilage fragments loaded in the 3D-printed PLA scaffold. **a** Schematic diagram of auricle model segmentation. **b** In vivo histological evaluation of the autologous ear cartilage fragments loaded in the 3D-printed PLA scaffold stained with H&E. PLA: polylactic acid; H&E: hematoxylin and eosin

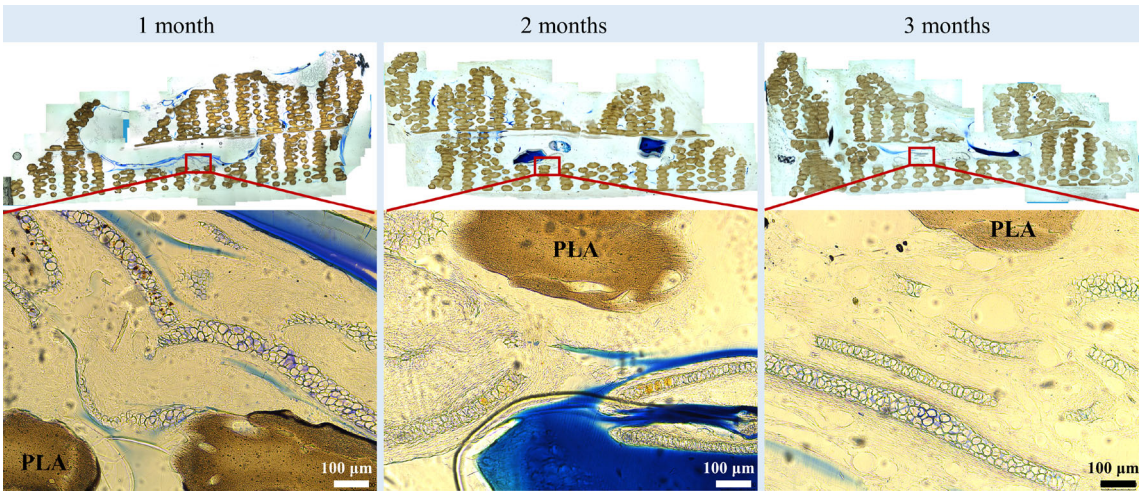

Fig. 8 In vivo histological evaluation of the autologous ear cartilage fragments loaded in the 3D-printed PLA scaffold stained with toluidine blue. PLA: polylactic acid

with 3D-printed scaffold for auricle repair is a simple and potential method that does not need to be expanded in vitro or with allografts. Therefore, this technology is economically and biologically attractive and reduces the conversion barriers in clinical application.

Conclusions

In this study, inspired by lawn transplantation, auricle cartilage fragments were loaded in 3D-printed auricle scaffolds to repair auricle defects. In vitro evaluation of hydrogel-coated cartilage fragments of different sizes showed that smaller sizes had better activity. The results of subcutaneous implantation experiments showed that the chondrocytes in the cartilage fragments indicated a round phenotype, and the cartilage matrix was maintained for three months. These results suggest that the combination of ear cartilage fragments and 3D-printed auricle scaffolds is of potential use for auricle reconstruction in the treatment of microtia.

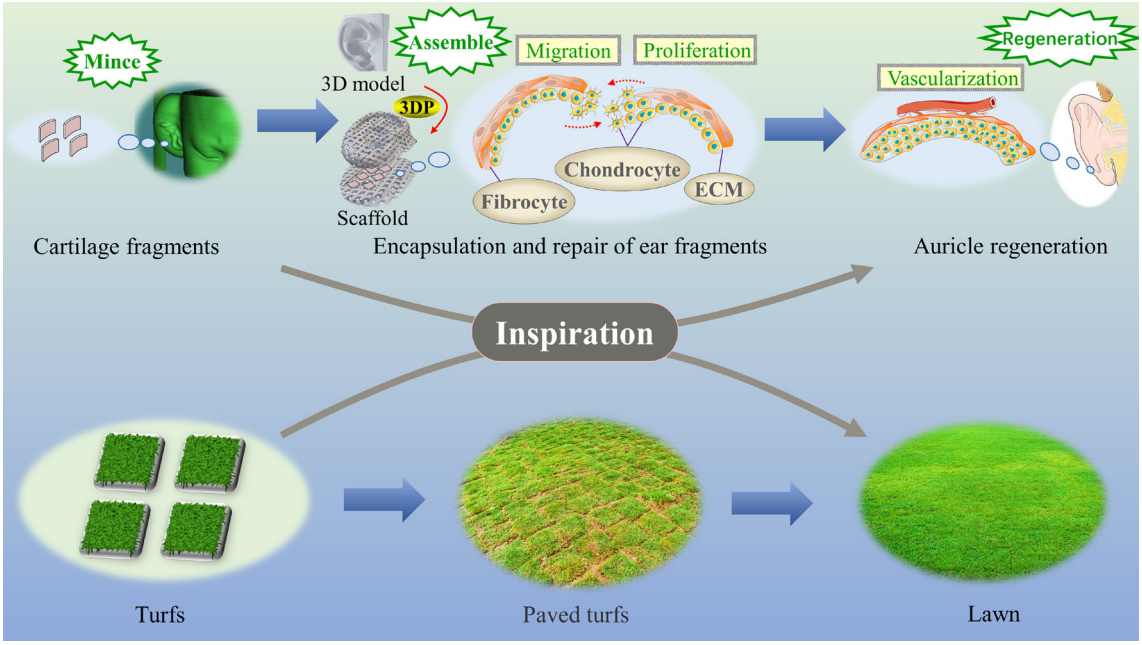

Fig. 9 The design of a 3D-printed auricle bracket encapsulating ear cartilage fragments to reconstruct the auricle was inspired by lawn transplantation. 3DP: 3D printing; ECM: extracellular matrix

Acknowledgements This work was supported by the National Natural Science Foundation of China (No. 81171731), the Project of Chengdu Science and Technology Bureau (Nos. 2021-YF05-01619-SN and 2021-RC05-00022-CG), the Science and Technology Project of Tibet Autonomous Region (Nos. XZ202202YD0013C and XZ201901-GB-08), the Sichuan Science and Technology Program (No. 2022YFG0066), and the 1·3·5 Project for Disciplines of Excellence, West China Hospital, Sichuan University (Nos. ZYJC21026, ZYGD21001 and ZYJC21077).

Author contributions CCZ, YJF and XDZ conceived and designed the experiments. XYG, PS and ZYP performed the experiments. LC and XJX prepared the figures. HRL and PT consulted the relevant literature. XYG, YXW and ZXS analyzed the data. QQK and ZYZ provided guidance on cell and animal experiments. XYG, PS and CCZ wrote the paper. YJF, ZYL and YC made revisions to the manuscript.

Declarations

Conflict of interest The authors declare that they have no conflict of interest.

Ethical approval All experiments were approved by the Animal Care and Use Committee of Sichuan University (KS2019022-2).

References

1. Kim HY, Jung SY, Lee SJ et al (2019) Fabrication and characterization of 3D-printed elastic auricular scaffolds: a pilot study. Laryngoscope 129(2):351–357. https://doi.org/10.1002/lary.27344
2. Fu YY, Li CL, Zhang JL et al (2019) Autologous cartilage microtia reconstruction: complications and risk factors. Int J Pediatr Otorhinolaryngol 116:1–6. https://doi.org/10.1016/j.ijporl.2018.09.035
3. Jovic TH, Stewart K, Kon M et al (2020) Auricular reconstruction: a sociocultural, surgical and scientific perspective. J Plast Reconstr Aesthet Surg 73(8):1424–1433. https://doi.org/10.1016/j.bjps.2020.03.025
4. Arshad M, Shirani G, Refoua S (2018) Rehabilitation of an auricular defect using surgical stent. World J Plast Surg 7(1):113–117
5. Han SE, Lim SY, Pyon JK et al (2015) Aesthetic auricular reconstruction with autologous rib cartilage grafts in adult microtia patients. J Plast Reconstr Aesthet Surg 68(8):1085–1094. https://doi.org/10.1016/j.bjps.2015.04.016
6. Bly RA, Bhrany AD, Murakami CS et al (2016) Microtia reconstruction. Facial Plast Surg Clin North Am 24(4):577–591. https://doi.org/10.1016/j.fsc.2016.06.011
7. Siegert R, Magritz R (2019) Otoplasty and auricular reconstruction. Facial Plast Surg 35(4):377–386. https://doi.org/10.1055/s-0039-1693745
8. Cenzi R, Farina A, Zuccarino L et al (2005) Clinical outcome of 285 medpor grafts used for craniofacial reconstruction. J Craniofac Surg 16(4):526–530. https://doi.org/10.1097/01.scs.0000168761.46700.dc
9. Jang CH, Koo Y, Kim G (2020) ASC/chondrocyte-laden alginate hydrogel/PCL hybrid scaffold fabricated using 3D printing for auricle regeneration. Carbohydr Polym 248:116776. https://doi.org/10.1016/j.carbpol.2020.116776
10. Uto S, Hikita A, Sakamoto T et al (2021) Ear cartilage reconstruction combining induced pluripotent stem cell-derived cartilage and three-dimensional shape-memory scaffold. Tissue Eng A 27(9–10):604–617. https://doi.org/10.1089/ten.TEA.2020.0106
11. Yue H, Pathak JL, Zou R et al (2021) Fabrication of chondrocytes/chondrocyte-microtissues laden fibrin gel auricular scaffold for microtia reconstruction. J Biomater Appl 35(7):838–848. https://doi.org/10.1177/0885328220954415
12. Hutmacher DW (2000) Scaffolds in tissue engineering bone and cartilage. Biomaterials 21(24):2529–2543. https://doi.org/10.1016/s0142-9612(00)00121-6

13. Langer R, Vacanti JP (1993) Tissue engineering. Science 260(5110):920–926. https://doi.org/10.1126/science.8493529
14. Kim S, Lee M (2020) Rational design of hydrogels to enhance osteogenic potential. Chem Mater 32(22):9508–9530. https://doi.org/10.1021/acs.chemmater.0c03018
15. Armiento AR, Alini M, Stoddart MJ (2019) Articular fibrocartilage—why does hyaline cartilage fail to repair? Adv Drug Deliv Rev 146:289–305. https://doi.org/10.1016/j.addr.2018.12.015
16. Kwak ES (2010) Asian cosmetic facial surgery. Facial Plast Surg 26(2):102–109. https://doi.org/10.1055/s-0030-1253497
17. Min SH, Kim JH, Lee MI et al (2020) Evaluation of auricular cartilage reconstruction using a 3-dimensional printed biodegradable scaffold and autogenous minced auricular cartilage. Ann Plast Surg 85(2):185–193. https://doi.org/10.1097/SAP.0000000000002313
18. Lee MR, Unger JG, Rohrich RJ (2011) Management of the nasal dorsum in rhinoplasty: a systematic review of the literature regarding technique, outcomes, and complications. Plast Reconstr Surg 128(5):538e–550e. https://doi.org/10.1097/PRS.0b013e31822b6a82
19. Gane S, East C, Jayaraj S et al (2007) Rolled auricular cartilage grafts for dorsal augmentation rhinoplasty. J Laryngol Otol 121(4):387–389. https://doi.org/10.1017/S0022215106003483
20. Lin AJ, Bernstein JL, Spector JA (2018) Ear reconstruction and 3D printing: is it reality? Current Surg Rep 6(2):4. https://doi.org/10.1007/s40137-018-0198-5
21. Song P, Hu C, Pei X et al (2019) Dual modulation of crystallinity and macro-/microstructures of 3D printed porous titanium implants to enhance stability and osseointegration. J Mater Chem B 7(17):2865–2877. https://doi.org/10.1039/c9tb00093c
22. Ma H, Feng C, Chang J et al (2018) 3D-printed bioceramic scaffolds: from bone tissue engineering to tumor therapy. Acta Biomater 79:37–59. https://doi.org/10.1016/j.actbio.2018.08.026
23. Long J, Zhang W, Chen Y et al (2021) Multifunctional magnesium incorporated scaffolds by 3D-printing for comprehensive postsurgical management of osteosarcoma. Biomaterials 275:120950. https://doi.org/10.1016/j.biomaterials.2021.120950
24. Zhu YZ, Joralmon D, Shan WT et al (2021) 3D printing biomimetic materials and structures for biomedical applications. Bio-Des Manuf 4(2):405–428. https://doi.org/10.1007/s42242-020-00117-0
25. Lee JS, Hong JM, Jung JW et al (2014) 3D printing of composite tissue with complex shape applied to ear regeneration. Biofabrication 6(2):024103. https://doi.org/10.1088/1758-5082/6/2/024103
26. Yin ZQ, Li D, Liu Y et al (2020) Regeneration of elastic cartilage with accurate human-ear shape based on PCL strengthened biodegradable scaffold and expanded microtia chondrocytes. Appl Mater Today 20:100724. https://doi.org/10.1016/j.apmt.2020.100724
27. Mukherjee P, Chung J, Cheng K et al (2021) Invitro and invivo study of PCL-hydrogel scaffold to advance bioprinting translation in microtia reconstruction. J Craniofac Surg 32(5):1931–1936. https://doi.org/10.1097/SCS.0000000000007173
28. Milazzo M, Negrini NC, Scialla S et al (2019) Additive manufacturing approaches for hydroxyapatite-reinforced composites. Adv Funct Mater 29(35):1903055. https://doi.org/10.1002/adfm.201903055
29. Wu L, Gu Y, Liu L et al (2020) Hierarchical micro/nanofibrous membranes of sustained releasing VEGF for periosteal regeneration. Biomaterials 227:119555. https://doi.org/10.1016/j.biomaterials.2019.119555
30. Montesdeoca CYC, Afewerki S, Stocco TD et al (2020) Oxygen-generating smart hydrogels supporting chondrocytes survival in oxygen-free environments. Colloids Surf B Biointerfaces 194:111192. https://doi.org/10.1016/j.colsurfb.2020.111192
31. De Moor L, Minne M, Tytgat L et al (2021) Tuning the phenotype of cartilage tissue mimics by varying spheroid maturation and methacrylamide-modified gelatin hydrogel characteristics. Macromol Biosci 21(5):e2000401. https://doi.org/10.1002/mabi.202000401
32. Ruiz-Cantu L, Gleadall A, Faris C et al (2020) Multi-material 3D bioprinting of porous constructs for cartilage regeneration. Mater Sci Eng C Mater Biol Appl 109:110578. https://doi.org/10.1016/j.msec.2019.110578
33. Arora A, Kothari A, Katti DS (2016) Pericellular plasma clot negates the influence of scaffold stiffness on chondrogenic differentiation. Acta Biomater 46:68–78. https://doi.org/10.1016/j.actbio.2016.09.038
34. Kapr J, Petersilie L, Distler T et al (2021) Human induced pluripotent stem cell-derived neural progenitor cells produce distinct neural 3D in vitro models depending on alginate/gellan gum/laminin hydrogel blend properties. Adv Healthc Mater 10(16):e2100131. https://doi.org/10.1002/adhm.202100131
35. Zhang BQ, Wang L, Song P et al (2021) 3D printed bone tissue regenerative PLA/HA scaffolds with comprehensive performance optimizations. Mater Des 201:109490. https://doi.org/10.1016/j.matdes.2021.109490
36. Wang C, Feng N, Chang F et al (2019) Injectable cholesterol-enhanced stereocomplex polylactide thermogel loading chondrocytes for optimized cartilage regeneration. Adv Healthc Mater 8(14):e1900312. https://doi.org/10.1002/adhm.201900312
37. Ishikawa S, Iijima K, Matsukuma D et al (2020) Enhanced function of chondrocytes in a chitosan-based hydrogel to regenerate cartilage tissues by accelerating degradability of the hydrogel via a hydrolysable crosslinker. J Appl Polym Sci 137(19):48893. https://doi.org/10.1002/app.48893
38. Salzmann GM, Ossendorff R, Gilat R et al (2021) Autologous minced cartilage implantation for treatment of chondral and osteochondral lesions in the knee joint: an overview. Cartilage 13(1_suppl):1124S–1136S. https://doi.org/10.1177/1947603520942952
39. Kim IL, Mauck RL, Burdick JA (2011) Hydrogel design for cartilage tissue engineering: a case study with hyaluronic acid. Biomaterials 32(34):8771–8782. https://doi.org/10.1016/j.biomaterials.2011.08.073
40. Huey DJ, Hu JC, Athanasiou KA (2012) Unlike bone, cartilage regeneration remains elusive. Science 338(6109):917–921. https://doi.org/10.1126/science.1222454
41. Van Gastel N, Stegen S, Eelen G et al (2020) Lipid availability determines fate of skeletal progenitor cells via SOX9. Nature 579(7797):111–117. https://doi.org/10.1038/s41586-020-2050-1
42. Bonasia DE, Marmotti A, Mattia S et al (2015) The degree of chondral fragmentation affects extracellular matrix production in cartilage autograft implantation: an in vitro study. Arthroscopy 31(12):2335–2341. https://doi.org/10.1016/j.arthro.2015.06.025
43. Lu Y, Dhanaraj S, Wang Z et al (2006) Minced cartilage without cell culture serves as an effective intraoperative cell source for cartilage repair. J Orthop Res 24(6):1261–1270. https://doi.org/10.1002/jor.20135
44. Bugbee W, Cavallo M, Giannini S (2012) Osteochondral allograft transplantation in the knee. J Knee Surg 25(2):109–116. https://doi.org/10.1055/s-0032-1313743
45. Zingler C, Carl HD, Swoboda B et al (2016) Limited evidence of chondrocyte outgrowth from adult human articular cartilage. Osteoarthritis Cartilage 24(1):124–128. https://doi.org/10.1016/j.joca.2015.07.014

46. Tsuyuguchi Y, Nakasa T, Ishikawa M et al (2021) The benefit of minced cartilage over isolated chondrocytes in atelocollagen gel on chondrocyte proliferation and migration. Cartilage 12(1):93–101. https://doi.org/10.1177/1947603518805205